HHS Public Access

Author manuscript

J Pediatr Surg. Author manuscript; available in PMC 2016 June 01.

Published in final edited form as:

J Pediatr Surg. 2015 June ; 50(6): 948–953. doi:10.1016/j.jpedsurg.2015.03.014.

The Effect of Impaired Angiogenesis on Intestinal Function Following Massive Small Bowel Resection

Jose Diaz-Miron, M.D.[1], **Raphael Sun, M.D.**[1], **Pamela Choi, M.D.**[1], **Joshua Sommovilla, M.D.**[1], **Jun Guo, Ph.D.**[1], **Christopher R. Erwin, Ph.D.**[1], **Junjie Mei, Ph.D.**[2], **G. Scott Worthen, M.D.**[2], and **Brad W. Warner, M.D.**[1]

[1]Division of Pediatric Surgery, St Louis Children's Hospital, Department of Surgery, Washington University School of Medicine, St Louis, MO

[2]Division of Neonatology, The Children's Hospital of Philadelphia, Philadelphia, PA

Abstract

Purpose—Intestinal adaptation involves villus lengthening, crypt deepening, and increased capillary density following small bowel resection (SBR). Mice lacking the proangiogenic chemokine CXCL5 have normal structural adaptation but impaired angiogenesis. This work evaluates the impact of incomplete adaptive angiogenesis on the functional capacity of the intestine after SBR.

Methods—CXCL5 knockout (KO) and C57BL/6 wild-type (WT) mice underwent 50% SBR. Magnetic resonance imaging measured weekly body composition. Intestinal absorptive capacity was evaluated through fecal fat analysis. Gene expression profiles for select macronutrient transporters were measured via RT-PCR. Postoperative crypt and villus measurements assessed for structural adaptation. Submucosal capillary density was measured through CD31 immunohistochemistry.

Results—Comparable postoperative weight gain occurred initially. Diminished weight gain, impaired fat absorption, and elevated steatorrhea occurred in KO mice after instituting high-fat diet. Greater postoperative upregulation of ABCA1 fat transporter occurred in WT mice, while PEPT1 protein transporter was significantly downregulated in KO mice. KO mice had impaired angiogenesis but intact structural adaptation.

Conclusion—After SBR, KO mice display an inefficient intestinal absorption profile with perturbed macronutrient transporter expression, impaired fat absorption, and slower postoperative weight gain. In addition to longer villi and deeper crypts, an intact angiogenic response may be required to achieve functional adaptation to SBR.

Correspondence: Brad W., Warner, M.D., St. Louis Children's Hospital, One Children's Place; Suite 5S40, St. Louis MO 63110, (314) 454-6022 - Phone, (314) 454-2442 – Fax, brad.warner@wustl.edu.

Keywords

CXCL5; Functional intestinal adaptation; Small bowel resection; Angiogenesis; High-fat diet

INTRODUCTION

Short gut syndrome (SGS) results from massive intestinal loss due to surgical resection in the treatment of conditions such as necrotizing enterocolitis (NEC), midgut volvulus, gastroschisis, or atresias. Following small bowel resection (SBR), the remnant bowel undergoes a series of architectural changes termed *adaptation*. This process involves critical and compensatory alterations that increase the intestinal absorptive area via increased enterocyte proliferation leading to the lengthening of villi and deepening of crypts [1–3]. In addition to these morphologic changes, we have previously reported resection-induced increased neovascularization within the adapted intestinal villi and submucosal compartments [4, 5]. This angiogenic response is preceded by increased expression of the chemokine C-X-C ligand 5 (CXCL5) protein [4, 6].

CXCL5 is a proangiogenic chemokine with neutrophil chemoattractive properties that recognizes and binds the CXCR2 receptor through a G-protein-coupled interaction. It has been shown to play a role in neutrophil homeostasis at mucosal sites and thus overexpressed in conditions such as NEC and inflammatory bowel disease [7–9]. Mice lacking this chemokine have normal structural features of adaptation, but lack the reactive angiogenesis after SBR [5].

The purpose of this study is to further expand on our previous observations in CXCL5 deficient mice to directly interrogate the impact of an incomplete angiogenic response on the functional capacity of the small intestine after massive SBR.

MATERIALS AND METHODS

Experimental design

This study was approved by the Washington University Animal Studies Committee (Protocol #20130038) and was in accordance with the National Institute of Health (NIH) laboratory animal care and use guidelines. C57BL/6 wild-type (WT) mice (n=9) and CXCL5 knockout (KO) mice (n=12) underwent a 50% SBR. Mice were then weighed regularly every 2–3 days for up to 35 days. Body composition measurements were performed using magnetic resonance imaging (MRI) once weekly until sacrifice. Fat absorption studies were performed during the week of postoperative day (POD) 14. Ileal tissue was harvested on either POD 21 for the short experimental arm or at POD 35 for the long-term arm. To assess for adaptation, villus height and crypt depth were measured via hematoxylin and eosin (H&E)-stained histology. Submucosal capillary density was measured by CD31-immunohistochemistry.

Animals

CXCL5 KO mice on a C57BL/6 background (Children's Hospital of Philadelphia, Philadelphia, Pennsylvania) [10] and non-mutant C57BL/6 WT mice (The Jackson Laboratory, Bar Harbor, ME) were used in the study [(age range 7–10 weeks; weight range 18.6 to 26.5 g (KO) and 22.5 to 26.8 g (WT)]. Animals were kept on a 12-hour light-dark schedule and were housed in a standard facility. The mice were given a liquid rodent diet (Micro-Stabilized Rodent Liquid Diet LD101; Purina Mills, St Louis, MO) 1 day prior to surgery.

Operative technique

Mice underwent a 50% proximal SBR as previously described [1]. Under isofluorane anesthesia, the bowel was eviscerated and transected 12 cm proximal to the ileocecal junction and 1 to 2 cm distal to the ligament of Treitz. The mesentery was ligated and the intervening bowel was removed. Intestinal continuity was restored through an end-to-end anastomosis using 9-0 monofilament sutures. Mice were provided water *ad libitum* for the first 24 hours, then fed with standard LD until POD 14, and finally switched to solid high-fat diet (HFD, Harlan Teklad TD.88137, 42% kcal fat) until sacrifice.

Body Composition Analysis

Lean body mass (LBM) and total body fat (BF) composition was recorded weekly on awake mice using MRI (EchoMRI 3–1, Echo Medical Systems).

Fat absorption studies

Following the introduction of HFD, mice were individually placed in metabolic cages during the week of POD 14. They were allowed to acclimate for 2 days before a 2–3 day period of food intake measurement and fecal collection. Feces were solubilized in water and extracted with a solution of 2:1 chloroform and methanol. Fecal lipid content was then determined gravimetrically and normalized to food consumption for determination of percent fat absorption [11].

Tissue harvest and enterocyte isolation

Mice were anesthetized with an intraperitoneal injection of ketamine, xylazine, and acepromazine (4:1:1). The eviscerated small bowel was flushed with ice-cold phosphate-buffered saline (PBS). The first 1 cm of bowel distal to the anastomosis was discarded. The next 2 cm segment was fixed in 10% neutral-buffered formalin for histology. On POD 21, animals in the short-term experimental arm had the next 10 cm transferred into containers with ice-cold PBS with protease inhibitors. Enterocyte isolation was performed as previously described through calcium chelation and mechanical dissociation for subsequent use in PCR analysis [12]. Animals were sacrificed via cervical dislocation.

Serum lipid profile analysis

Blood was collected via cardiac puncture on POD 21 (WT n=8; KO n=9). Serum total cholesterol and triglyceride (TG) concentrations were determined using Infinity total

cholesterol and TG kits (Fischer Scientific, Pittsburg, PA). Serum free fatty acids (FFA) were determined using the NEFA C kit (Wako Chemicals, Richmond, VA).

RT-PCR determination of gene expression profiles

RNA was extracted from ileal tissue using the RNAqueous kit (Ambion, Austin TX) (WT n=8; KO n=9). A TaqMan RNA-to Ct 1-Step kit (Applied Biosytems, Foster city, CA) was used to determine relative gene expression directly from the isolated RNA. Equal amounts of RNA were used for real-time PCR with β-actin as endogenous control and a whole bowel standard sample used as calibrator. Gene expression profiles for CXCL5 as well as for select fat [CD36, microsomal triglyceride transfer protein (MTTP), apolipoprotein B (APOB), ATP-binding cassette, sub-family A, member 1 (ABCA1), diacylglycerol O-acyltransferase 2 (DGAT2), and ATP-binding cassette, sub family G, member 5 (ABCG5)] and protein [peptide transporter 1 (PEPT1)] transporters were examined using the corresponding primers, reagents, and with a 750 Fast Real-Time PCR instrument (Applied Biosystems, Foster City, CA).

Evaluation of structural adaptation

Villus height and crypt depth were measured on H&E stained sections by a blinded investigator using MetaMorph software (Dowington, PA). At least twenty well-oriented villi and crypts per animal were measured at 10x magnification.

Measurements of submucosal capillary density

Slides were deparaffinized in xylene and rehydrated in gradients of ethanol. Antigen retrieval was carried out in DIVA solution (BioCare, Bedford Park, IL). Primary antibody to CD31 (Abcam, Cambridge, MA) was diluted in DaVinci Green (BioCare, Bedford Park, IL) and incubated overnight. Slides were then incubated at RT with a conjugated polymer probe in PBS with Tween 20 (PBST). HRP conjugated probe (Mach 2 Rabbit HRP, BioCare, Bedford Park, IL) was diluted in PBST (BioCare, Bedford Park, IL) and incubated at RT. Slides were developed with 3,3′-diaminobenzidine (Sigma-Aldrich, St. Louis, MO), washed in distilled water, and counterstained with hematoxylin. CD31-stained submucosal vessels of the small intestine were counted under light microscopy at 40x magnification by a blinded investigator. At least 10 well-oriented fields per animal were considered for analysis.

Statistical analysis

Values are presented as mean ± SEM. Sigma Stat statistical package (SPSS, Chicago, IL) was used for all statistical analyses. Student’s t-test was used for comparisons of two groups while ANOVA was used for comparisons of more than two groups. A p-value of less than 0.05 was considered significant.

RESULTS

CXCL5 KO mice have impaired postoperative weight gain

Mice were standardized to their respective baseline weight and reported as a relative weight percentage in relation to this measurement. Groups mostly exhibited comparable postoperative weight gain while on LD. Diminished weight gain was observed in the KO group after instituting a HFD (Figure 1A). There were no noted differences in percent BF or LBM composition between the groups, as measured by MRI. Massive SBR and HFD, however, led to a significant reduction in percent LBM with concomitant increase in the percent BF composition among all mice (Figure 1B, C). This unique metabolic response has been previously established by our group [13].

Food intake and stool output were measured at four different time points after the institution of HFD and reported as either grams of ingested food or grams of fecal output per mouse body weight in grams. Both WT and KO mice had similar food intake (0.15 ±0.013 vs. 0.13 ±0.009, p=0.201) and fecal output (0.013 ±0.001 vs. 0.011 ±0.001, p=0.098) during the experiment.

CXCL5 KO mice display greater impairment in fat absorption after SBR

Preoperatively, fat absorption was similar between CXCL5 KO and WT mice (95.13% ±0.91 vs. 93.32% ±0.74, p=0.163) on HFD. Following SBR, and after the reinstitution of HFD, CXCL5 KO mice had significantly reduced fat absorption (90.26% ±0.58 vs. 92.16% ±0.55, p=0.027) and greater steatorrhea (18.38% ±1.21 SEM vs. 14.01% ±0.88 SEM, p=0.006).

CXCL5 KO mice have lower postoperative circulating serum FFA

At baseline, both CXCL5 WT and KO mice had similar levels of circulating serum TG, FFA, and total cholesterol. Serum collected on POD 21 revealed no statistical change in TG when compared to baseline. The WT group had significant upregulation of FFA levels from baseline. Total serum cholesterol significantly increased in both groups at comparable levels (Figure 2).

CXCL5 KO and WT mice have normal structural adaptation

Structural adaptation occurred normally in both CXCL5 KO and WT mice after SBR, as evident by comparable postoperative percent increases in villus height (25.09% ±5.3% vs. 29.07% ±5.5%, p=0.904).

CXCL5 KO mice exhibit an impaired angiogenic response after SBR

Results of submucosal CD31 capillary counts were consistent with our previous studies. Impaired angiogenesis occurred exclusively in the CXCL5 KO group after SBR (Figure 3). Compared with historical control data, CXCL5 KO mice had equivalent angiogenic measurements as WT mice after sham operations (small bowel transection and reanastomosis; data not shown).

CXCL5 KO mice display a perturbed gene expression profile of select macronutrient transporters

Gene expression profiles for select fat (CD36, MTTP, APOB, ABCA1, DGAT2, and ABCG5) and protein (PEPT1) transporters in isolated intestinal villus cells were measured using RT-PCR at POD 21 (WT n=6; KO n=7) and reported as the fold change from baseline values. No basal differences were noted between the groups. Significant and comparable upregulation from baseline were noted in CD36, MTTP, and ABCG5 levels among the experimental groups after SBR. Postoperative upregulation of the ABCA1 fat transporter was more pronounced in WT mice (p=0.029), while PEPT1, the major protein transporter, was significantly downregulated only in the KO group (p=0.018) (Figure 4). Additionally, mRNA isolated from intestinal villus from CXCL5 KO and WT mice confirmed that CXCL5 mRNA was absent only in the KO mice (data not shown).

DISCUSSION

In the present study we identified possible clinical implications of CXCL5 after SBR. CXCL5 KO mice were noted to achieve normal features of structural adaptation, without the robust angiogenic response seen in WT controls. KO mice also display features of impaired small intestinal absorptive capacity following the institution of a HFD.

Angiogenesis is involved in several physiologic and pathologic conditions of increased cellular proliferation such as wound healing, development, and neoplasia [14–17]. This process is also seen within the small intestine after SBR in both the lamina propria of the adapted villus and submucosal compartment [4, 5]. We have previously been able to hinder this angiogenic response through the selective blockade of salivary-derived vascular endothelial growth factor (VEGF), resulting in adaptive impairment [18]. In the current study, however, impairment of angiogenesis in CXCL5 KO mice after SBR did not alter the structural features of adaptation, suggesting an uncoupling of the stimulus for enterocyte proliferation from that of angiogenesis. This uncoupling is further supported by studies detecting enterocyte proliferation as early as POD 3, prior to the onset of a detectable angiogenic response [4]. Collectively, these findings would support the notion that angiogenesis occurs in response to the need for providing greater nutrient to the adapting bowel, as opposed to being the primary adaptive growth stimulus.

Body composition changes observed in the study were in accordance with previously reported postoperative phenotypes [13, 19]. After SBR, mice exhibit increased adiposity and decreased percent LBM while on HFD. Interestingly, these observations persist even in the absence of HFD introduction [13]. This postoperative phenotype may represent an innate stress response to massive intestinal resection and to an overall nutrient deprivation phenomenon.

CXCL5 KO mice without a resection-induced angiogenic response after SBR display an inefficient fat absorption phenotype, as evident by lower percent fat absorption measurements and steatorrhea. These KO mice also have aberrancies in select macronutrient transporter profiles, as measured by RT-PCR. The fat transporters evaluated (CD36, MTTP, APOB, ABCA1, DGAT2, ABCG5) were selected based on familiarity due to our previous

experiments. PEPT1 was selected based on its implication as a major mechanism for intestinal protein absorption [21]. While we noted a significant downregulation in this protein transporter among KO mice, additional nitrogen balance studies could have further developed this observation.

With the exception of APOB and DGAT2, the evaluated fat transporters were significantly upregulated in both groups following the institution of HFD. ABCA1 transporter, however, was upregulated significantly more in WT than KO mice. While intestinal fat absorption is a highly complex process involving many biochemical processes and transporters, this suggests a potential involvement of the ABCA1 transporter in the impaired fat absorption phenotype exhibited by CXCL5 deficient mice. ABCA1 is a member of the ATP-binding cassette transporter family that is required for the formation of HDL in the plasma [22]. In Tangier disease, ABCA1 mutations lead to a metabolic derangement involving severe HDL deficiency, elevated serum TG, deposition of sterol in tissues, and premature coronary atherosclerosis [22]. While we did not find differences in total cholesterol between the groups following SBR and HFD introduction, evaluation of serum HDL and LDL fractions would have provided additional insight into the malabsorptive phenotype of the KO group. Altered postoperative serum FFA in CXCL5 KO mice may serve as a possible explanation for the variations in this intestinal transporter expression. Recent studies have shown that dietary FFAs may alter the metabolism and formation of HDL through modulation of ABCA1 expression [23].

In this study we believe the putative reason for the impaired functional intestinal capacity in CXCL5 KO mice is their inadequate angiogenic response to SBR. We believe that in order to achieve total parenteral nutrition independence, SGS patients not only require a critical length of residual bowel and a robust intestinal adaptive reaction, but also an intact angiogenic response. The interplay of these phenomena, however, requires further investigation to establish causal and mechanistic relationships. Resection-induced neovascularization may be critical to support the higher metabolic demands required for increased enterocyte proliferation and subsequent architectural changes that happen in the intestine. Additionally, this adaptive reaction may improve the absorptive efficiency of the newly adapted small bowel by serving as additional transport channels for luminal to basolateral macronutrient traffic.

Acknowledgments

This work was supported by the St. Louis Children’s Hospital Foundation Children’s Surgical Sciences Research Institute, NIH Grants T32 DK077653 (Diaz-Miron), P30DK52574 (Digestive Diseases Research Core Center, Washington University School of Medicine), and P60DK20579 (Diabetes Models Phenotyping Core, Washington University School of Medicine).

References

1. Helmrath MA, VanderKolk WE, Can G, et al. Intestinal adaptation following massive small bowel resection in the mouse. J Am Coll Surg. 1996; 183:441–449. [PubMed: 8912612]
2. McDuffie LA, Bucher BT, Erwin CR, et al. Intestinal adaptation after small bowel resection in human infants. J Pediatr Surg. 2011; 46:1045–1051. [PubMed: 21683196]

3. Taylor JA, Martin CA, Nair R, et al. Lessons learned: optimization of a murine small bowel resection model. J Pediatr Surg. 2008; 43:1018–1024. [PubMed: 18558176]
4. Martin CA, Perrone EE, Longshore SW, et al. Intestinal resection induces angiogenesis within adapting intestinal villi. J Pediatr Surg. 2009; 44:1077–1082. discussion 1083. [PubMed: 19524720]
5. Rowland KJ, Diaz-Miron J, Guo J, et al. CXCL5 is Required For Angiogenesis, but not Structural Adaptation after Small Bowel Resection. J Pediatr Surg. 2014
6. McMellen ME, Wakeman D, Erwin CR, et al. Epidermal growth factor receptor signaling modulates chemokine (CXC) ligand 5 expression and is associated with villus angiogenesis after small bowel resection. Surgery. 2010; 148:364–370. [PubMed: 20471049]
7. Mei J, Liu Y, Dai N, et al. Cxcr2 and Cxcl5 regulate the IL-17/G-CSF axis and neutrophil homeostasis in mice. J Clin Invest. 2012; 122:974–986. [PubMed: 22326959]
8. Z'Graggen K, Walz A, Mazzucchelli L, et al. The C-X-C chemokine ENA-78 is preferentially expressed in intestinal epithelium in inflammatory bowel disease. Gastroenterology. 1997; 113:808–816. [PubMed: 9287972]
9. MohanKumar K, Kaza N, Jagadeeswaran R, et al. Gut mucosal injury in neonates is marked by macrophage infiltration in contrast to pleomorphic infiltrates in adult: evidence from an animal model. Am J Physiol Gastrointest Liver Physiol. 2012; 303:G93–102. [PubMed: 22538401]
10. Mei J, Liu Y, Dai N, et al. CXCL5 regulates chemokine scavenging and pulmonary host defense to bacterial infection. Immunity. 2010; 33:106–117. [PubMed: 20643340]
11. Schwarz M, Lund EG, Setchell KD, et al. Disruption of cholesterol 7alpha-hydroxylase gene in mice. II. Bile acid deficiency is overcome by induction of oxysterol 7alpha-hydroxylase. J Biol Chem. 1996; 271:18024–18031. [PubMed: 8663430]
12. Guo J, Longshore S, Nair R, et al. Retinoblastoma protein (pRb), but not p107 or p130, is required for maintenance of enterocyte quiescence and differentiation in small intestine. J Biol Chem. 2009; 284:134–140. [PubMed: 18981186]
13. Tantemsapya N, Meinzner-Derr J, Erwin CR, et al. Body composition and metabolic changes associated with massive intestinal resection in mice. J Pediatr Surg. 2008; 43:14–19. [PubMed: 18206448]
14. Addison CL, Daniel TO, Burdick MD, et al. The CXC chemokine receptor 2, CXCR2, is the putative receptor for ELR+ CXC chemokine-induced angiogenic activity. J Immunol. 2000; 165:5269–5277. [PubMed: 11046061]
15. Keeley EC, Mehrad B, Strieter RM. Chemokines as mediators of neovascularization. Arterioscler Thromb Vasc Biol. 2008; 28:1928–1936. [PubMed: 18757292]
16. Risau W. What, if anything, is an angiogenic factor? Cancer Metastasis Rev. 1996; 15:149–151. [PubMed: 8842485]
17. Folkman J. Is angiogenesis an organizing principle in biology and medicine? J Pediatr Surg. 2007; 42:1–11. [PubMed: 17208533]
18. Parvadia JK, Keswani SG, Vaikunth S, et al. Role of VEGF in small bowel adaptation after resection: the adaptive response is angiogenesis dependent. Am J Physiol Gastrointest Liver Physiol. 2007; 293:G591–598. [PubMed: 17585015]
19. Wang Y, Iordanov H, Swietlicki EA, et al. Targeted intestinal overexpression of the immediate early gene tis7 in transgenic mice increases triglyceride absorption and adiposity. J Biol Chem. 2005; 280:34764–34775. [PubMed: 16085642]
20. Yu C, Jiang S, Lu J, et al. Deletion of Tis7 protects mice from high-fat diet-induced weight gain and blunts the intestinal adaptive response postresection. J Nutr. 2010; 140:1907–1914. [PubMed: 20861213]
21. Adibi SA. The oligopeptide transporter (Pept-1) in human intestine: biology and function. Gastroenterology. 1997; 113:332–340. [PubMed: 9207295]
22. Parks JS, Chung S, Shelness GS. Hepatic ABC transporters and triglyceride metabolism. Curr Opin Lipidol. 2012; 23:196–200. [PubMed: 22488425]
23. Lee J, Park Y, Koo SI. ATP-binding cassette transporter A1 and HDL metabolism: effects of fatty acids. J Nutr Biochem. 2012; 23:1–7. [PubMed: 21684139]

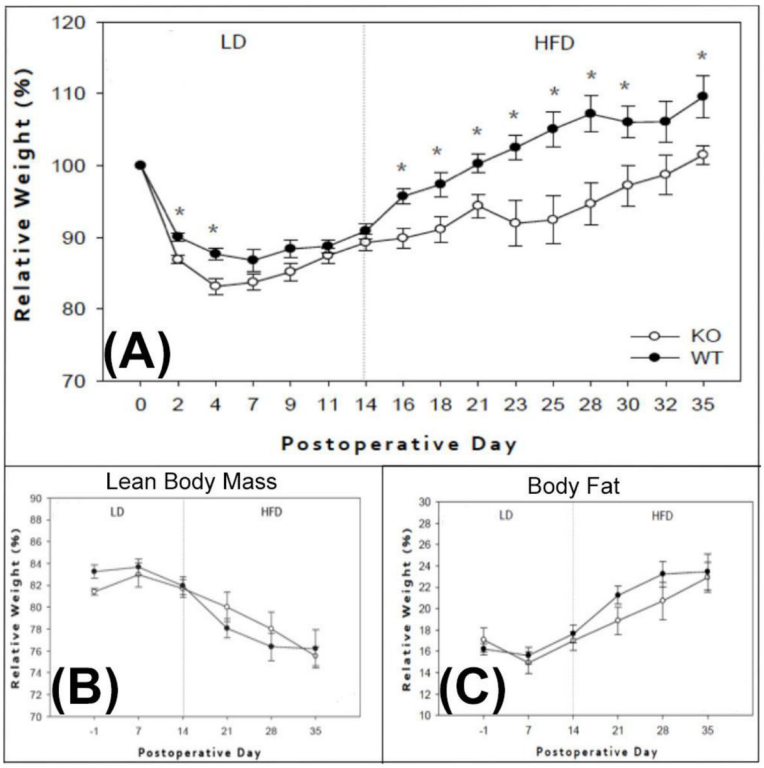

Figure 1. Postoperative weight gain and body composition measurements

(A) Percent weight change between WT (black circles) and CXCL5 KO (white circles) mice on the indicated POD; asterisks indicate $p<0.05$. Percent lean body mass **(B)** and body fat **(C)** between WT and KO mice measured through MRI; no significant differences were detected between groups. LD=liquid diet; HFD=High-fat diet. \

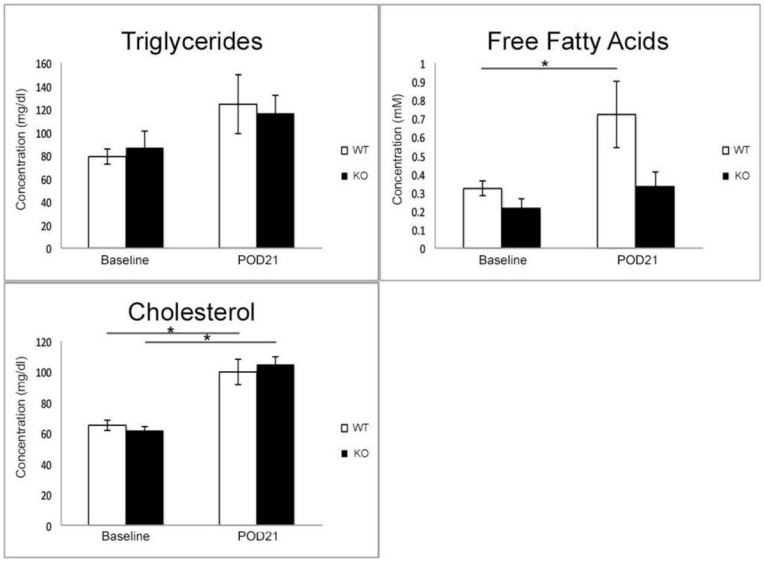

Figure 2. Postoperative serum lipid profile

Serum collected at baseline and on POD 21 was analyzed for total circulating levels of triglycerides, free fatty acids, and cholesterol. No differences were observed in lipid profiles between groups at baseline. Serum triglycerides did not increase significantly from preoperative values in both WT and KO mice. Free fatty acid levels significantly increased on POD 21 in the WT group, but not in the CXCL5 KO mice. Significant increase from baseline was noted in total cholesterol in both WT and KO mice. Asterisk denote significant differences with $p<0.03$.

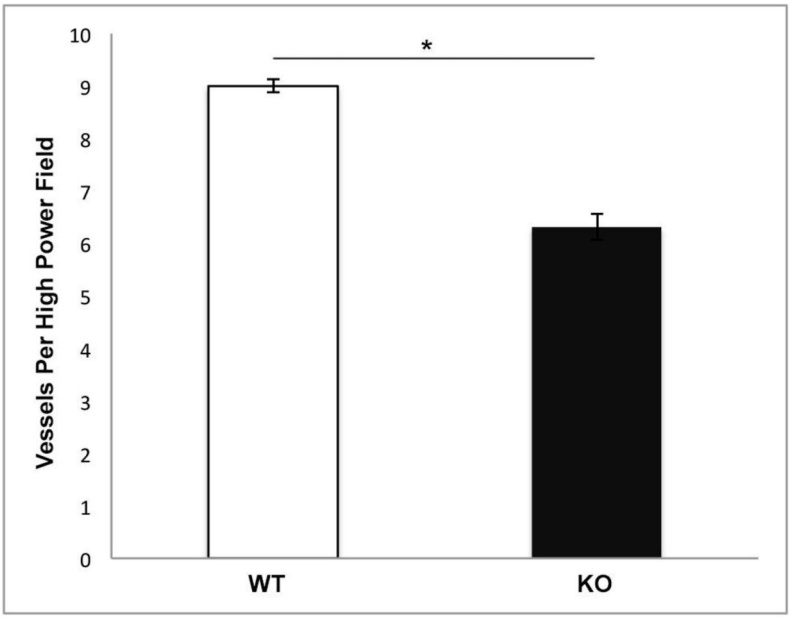

Figure 3. Number of CD31-positive submucosal vessels

Submucosal capillary counts per high power field (40x) magnification revealed impaired angiogenesis in the CXCL5 KO mice after SBR (*$p<0.001$).

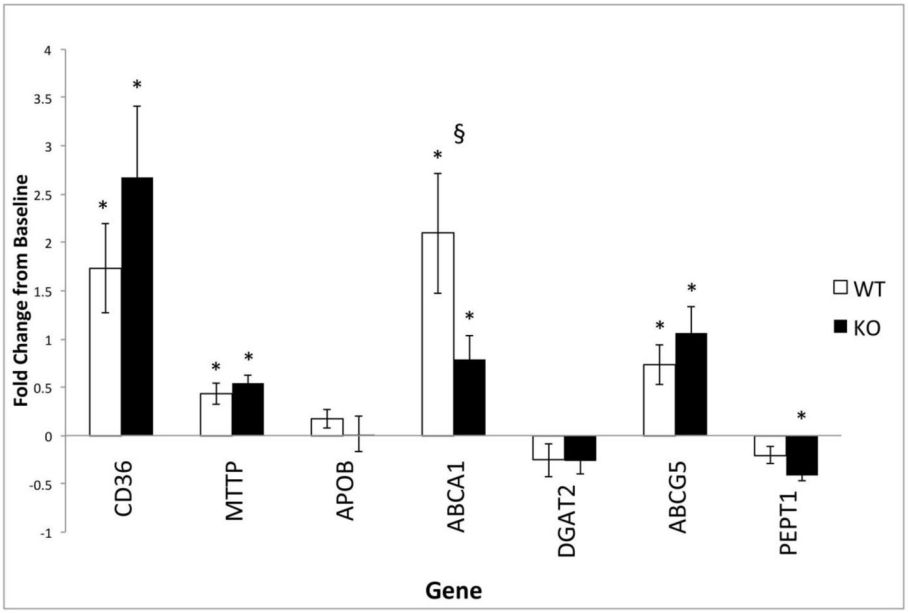

Figure 4. Macronutrient transporter profile in WT and CXCL5 KO mice after SBR

Postoperative upregulation of the ABCA1 fat transporter was more pronounced in WT mice (§=$p<0.03$), while PEPT1, the major protein transporter, was downregulated only significantly in the KO group. Reported as the fold changes from non-operated baseline control values at POD 21. Asterisks indicate significant change from baseline value within each group ($p<0.05$).